Seasonal variability and regulation of methane and sulfate fluxes in Baltic Sea estuarine sediments

Joanna E. Sawicka and Volker Brüchert

Department of Geological Sciences, Stockholm University, Stockholm, 10691, Sweden

Correspondence to: Volker Brüchert (volker.bruchert@geo.su.se)

Abstract. Marine methane emissions originate largely from near-shore and coastal systems, but emission estimates are often not based on temporally well-resolved data or sufficient understanding of the variability of methane consumption and production processes in the underlying sediment. The objectives of our investigation were to explore the effects of seasonal temperature, changes in benthic oxygen concentration, and historical eutrophication on sediment methane concentrations and benthic fluxes at two type localities for open-water coastal and eutrophic, estuarine sediment in the Baltic Sea. Benthic fluxes of methane and oxygen, sediment porewater concentrations of dissolved sulfate, methane, and ^{35}S-sulfate reduction rates were obtained over a 12-month period from April 2012 to April 2013. Benthic methane fluxes varied by factors of 5 and 12 at the offshore coastal site and the eutrophic estuarine station, respectively, ranging from 0.1 mmol $m^{-2}d^{-1}$ in winter at an open coastal site to 2.6 mmol $m^{-2}d^{-1}$ in late summer in the inner eutrophic estuary. Total oxygen uptake (TOU) and ^{35}S-sulfate reduction rates (SRR) correlated with methane fluxes showing low rates in the winter and high rates in the summer. The highest porewater methane concentrations also varied by factors of 6 and 10 over the sampling period with lowest values in the winter and highest values in late summer-early autumn. The highest porewater methane concentrations were 5.7 mM a few centimeters below the sediment surface, but never exceeded the in-situ saturation concentration. About 20 % of the total sulfate reduction was coupled to anaerobic methane oxidation lowering methane concentrations below the sediment surface far below the saturation concentration. These data imply that bubble emission likely plays no or only a minor role for methane emissions in these sediments. The changes in porewater methane concentrations over the observation period were too large to be explained by temporal changes in methane formation and methane oxidation rates due to temperature alone. Additional factors such as regional and local hydrostatic pressure changes and coastal submarine groundwater flow may also affect the vertical and lateral transport of methane.

Keywords **Methane cycling, coastal and estuarine sediment, seasonality**

1 Introduction

The world's estuaries have been suggested to emit between 1.8 and 6.6 Tg CH_4 y^{-1} to the atmosphere (Borges and Abril, 2011; Amouroux et al 2002, Marty et al., 2001; Middelburg et al., 2002; Sansone et al., 1999; Upstill-Goddard et al., 2000), a potentially considerable portion of the estimated total oceanic emissions of 10-30 Tg CH_4 y^{-1} (Judd, 2004; Etiope et al., 2008; Kirschke et al., 2013). As other globally upscaled estimates of emissions, these estimates also have considerable uncertainties. In the case of estuaries, a major cause of the uncertainty are relatively few spatially and temporally resolved measurements of anaerobic carbon degradation measurements in sediments and measurements of methane fluxes from sediments. In estuarine waters methane is produced by methanogenesis in underlying anoxic sediments, lateral freshwater or sewage discharge, seepage of methane-rich groundwater, or transport in the near-shore by aquatic plants (Borges and Abril, 2011). The amount of sedimentary methane production in estuaries is a function of organic matter availability, bottom water oxygen concentrations, and the salinity of the estuary. Methane production is generally greater in low-salinity estuaries because of lower sulfate availability to promote bacterial sulfate reduction (Borges and Abril, 2011). Methane fluxes from estuarine sediments are characterized by significant spatial and temporal variability (Borges and Abril 2011). Temporal patterns show that concentrations and fluxes of CH_4 are generally higher in the warmer season and low in the colder season (Crill et al., 1983, Martens and Klump, 1984, Musenze et al., 2014; Reindl and Bolałek, 2014). Notably, very few studies have considered CH_4 fluxes in high-latitude environments during snow- and ice-covered periods. While shallow systems within the tidal range derive a significant amount of the methane flux from ebullition (Martens and Klump, 1984), groundwater discharge, tidal pumping, and transport by aquatic plants (Middelburg et al., 2002; Kristensen et al 2008), the transport from deeper

systems such as fjords and fjärds is thought to occur largely by molecular diffusion (Abril and Iversen, 2002, Sansone et al., 1998).

Globally more than 90% of methane produced in marine sediments is estimated to be oxidized by the anaerobic oxidation of methane (AOM), mostly in the sulfate-methane transition zone (Knittel and Boetius, 2009, Martens and Berner, 1974; Jørgensen and Parkes, 2010). It is not known how much methane is oxidized by AOM in estuarine sediments. In addition, up to 90% of the remaining methane that reaches the sediment surface may be oxidized aerobically at the sediment surface or in the water column (Reeburgh, 2007). Yet, methane concentrations in estuarine waters are almost always higher than the atmospheric equilibrium concentration indicating that microbial oxidation processes and physical exchange with the atmosphere in estuaries are relatively inefficient in removing methane. Despite its obvious importance, only few studies have specifically addressed anaerobic oxidation of methane by sulfate and aerobic oxidation in estuarine environments (e.g., Treude et al., 2005, Thang et al., 2013).

The objective of this study was therefore to further elucidate mechanisms behind temporal variability of methane fluxes in a high-latitude coastal and estuarine environment with strong seasonal temperature variability, winter ice cover, and variable degree of eutrophication stress. These data fill an important gap of global inventories of nearshore sediment methane dynamics and help improve our mechanistic understanding of methane emissions from marine near-shore systems. We determined porewater concentrations of methane and sulfate, measured sulfate reduction rates with the ^{35}S-sulfate tracer method, and conducted core incubations to determine benthic fluxes of methane and oxygen at two deep stations of a low-salinity Baltic Sea estuary inside and at the opening of the estuary to the Baltic. Investigations were carried out over four seasons to capture the variability of chemical and biological conditions at the sediment surface and their influence on methane dynamics.

2 Materials and methods

2.1 Site description

Himmerfjärden (Figure 1) is a fjord-type estuary with a surface area of 174 km^2 and a N-S salinity gradient increasing from 5.5‰ in the inner part to 7.0‰ at the opening to the Baltic. It is morphologically characterized by four basins, divided by sills and has a low flushing rate (~0.025/day) (Savage and Elmgren, 2010). In 2012, the freshwater discharge comprised land run-off and precipitation (30% and 21% respectively), outflow from Lake Mälaren in the north (19%) and the river Trosaån (23%), and discharge from a sewage treatment plant (6%) (Larsson et al., 2012). The sewage treatment plant, built in the early 1970s, treats sewage water from ca. 314,000 inhabitants of the southern Stockholm metropolitan area, and its inorganic effluent is discharged mainly in the form of inorganic nitrogen and phosphorus to the inner basins (Savage and Elmgren, 2010). In 2012, the sewage treatment contributed 45% of the total phosphorus and 57% of the total inorganic nitrogen discharge to the northern Himmerfjärden area (Larsson et al., 2012) and discharged 1676 tons carbon (measured as chemical oxygen demand COD) (Stridh, 2012). The estuary undergoes thermohaline stratification during late summer and autumn, especially in the inner part, which experiences regular seasonal bottom water hypoxia. The tidal range is low (few cm) and relatively cold bottom waters (1.5 - 9°C) dominate throughout the year. Water level can vary annually by about 50 cm depending on local wind and hydrographic conditions. Late-summer-early fall bottom water hypoxia has also been reported occasionally for the outer basins of the estuary when winds are weak and circulation is inhibited (Elmgren and Larsson, 1997). Sedimentation areas in Himmerfjärden can be divided into accumulation and transport bottoms (Jonsson et al., 2003). About 21% of the sediment surface in Himmerfjärden is

129 classified as accumulation bottoms of particulate material and receives 3.3-9 mol C m^{-2} y^{-1}
130 (Karlsson et al., 2010; Thang et al., 2013).
131 Bottom water and sediment samples were taken from a station in the inner part of
132 Himmerfjärden, station H6, and from a station located outside the estuary, station B1 (Figure
133 1). Samples were collected in April, August, October 2012, and in February 2013. In addition,
134 in April 2013 whole-core incubations were performed to determine methane and oxygen
135 fluxes to record a full year of seasonal variability. Station B1 has soft, olive grey, muddy
136 sediment with a 1-2 cm-thick rusty brown surface layer, while the sediment at station H6 is
137 soft, laminated black mud with a 1-2 mm thin brown surface layer that occurred only during
138 the winter and spring. Sediment accumulation rates range from 0.98 cm yr^{-1} in the innermost
139 part of the estuary to 0.77 cm yr^{-1} in the outer part of the estuary (Thang et al., 2013).
140

141 **2.2 Sample collection**

142 Sediments with well-preserved sediment surfaces were collected with a Multicorer in acrylic
143 tubes (9.5 cm diameter) to 40 cm depth to determine ^{35}S-sulfate reduction rates, porosity, and
144 the porewater constituents methane and sulfate. Additional cores were collected for sediment
145 core incubations. Porewater methane samples were immediately collected on-board from the
146 cores as described below. The other cores were capped with rubber stoppers, transported to
147 the marine laboratory on the island of Askö within 90 minutes and kept cold at bottom water
148 temperatures for later experiments and subsampling. In February 2013, ice partially covered
149 station B1 and there was complete ice cover at station H6, and sampling was only possible
150 after ice breaking. For whole-core incubations, 30 l of bottom water was collected with a 5
151 liter HydroBios bottle and kept cold until for the experiments. Temperature, salinity, and
152 oxygen concentrations were determined with a handheld WTW Oxygen meter directly in the
153 water overlying the sediment cores.

2.3 Organic carbon concentrations and porosity

Surface sediment concentrations of organic carbon were determined on freeze-dried sediment with a Fisons CHN elemental analyzer after treatment of freeze-dried sediment with 1M HCl to remove inorganic carbon. Water content (%) was determined by drying 5 mL of sediment at 105°C for two hours and calculating the percent loss after drying.

2.4 Methane analysis

Samples for methane were collected directly through the side of taped, pre-drilled core liners and taken in 2-cm intervals minutes after the core was retrieved on deck. The core sampling method used in this study permits complete sampling and preservation of porewater methane within 5 minutes after the core was on deck. Under these circumstances, loss of methane due to gas loss is low and methane concentrations could be determined for porewaters that were far above the saturation limit at 1 atmosphere pressure for the salinity and temperature range of the bottom water (between 1.9 mM and 2.4 mM). A sediment sample of exactly 2.5 mL was taken with a 3 mL cut-off syringe. The sample was transferred to a 20 mL serum vial containing 5 mL 5 M NaCl and immediately closed with a thick septum and an aluminum crimp seal. The sample was shaken and 5 mL of brine was injected into a sample vial to displace 5 mL gas out of a vial into the syringe. The CH_4 measurements were carried out on a gas chromatograph (GC) with a flame ionization detector (FID) (SRI 8610C) after separation on a 3 feet Porapak Q pre-column before a 9 feet Hayesep D column with N_2 as carrier gas. CH_4 standards 100 ppm, 1000ppm, and 10000 ppm (Air Liquide) were used for calibration.

The concentration of methane (mM) of a sample was calculated as follows:

$$CH_4(mM) = \frac{CH_{4\ hsp} \cdot V_{hsp}}{1000 \cdot 24.148 \cdot V_{sed} \cdot \rho} \quad (1)$$

where $CH_{4_{hsp}}$ is the concentration of methane in the headspace of the sample vial (ppm), V_{hsp} is the volume of the headspace (L), V_{sed} is the volume of the sediment sample (L), ρ is sediment porosity, and 24.148 (L mol^{-1}) is the molar volume of gas at standard pressure 100 kPa and 298 K.

2.5 Sulfate concentration

Porewater samples for sulfate concentration measurements were obtained using rhizones (Atlas Copco Welltech) (Seeberg-Elverfeldt et al. 2005). Rhizones were treated for 2 hours in 1M HCl, followed by two rinses with deionized water for 2 hours and final storage in deionized water. Rhizones were connected to 10 mL disposable plastic syringes via 3-way luerlock stopcock and inserted in 1-cm intervals through tight-fitting, pre-drilled holes in the liner of the sediment cores. The first mL of pore water was discarded from the syringe. No more than 2 mL were collected from each core to prevent cross-contamination of adjacent intervals (Seeberg-Elverfeldt et al., 2005). Sulfate concentrations were determined with a Dionex System IC 20 ion chromatograph.

2.6 ^{35}S-Sulfate reduction rates

To determine bacterial sulfate reduction rates (SRR) sediment cores were subsampled in 40-cm long 28 mm-diameter cores with 1-cm spaced, silicon-sealed, pre-drilled small holes on the side for injections. For the incubation, the whole-core incubation method by Jørgensen (1978) was used. $^{35}SO_4^{2-}$ tracer solution was diluted in a 6 ‰ NaCl solution containing 0.5 mM SO_4^{2-} and 2.5 µL of the tracer solution (50kBq) was injected through the pre-drilled

holes. The cores were then capped and sealed in plastic wrap foil and incubated for 8 hours at the respective bottom water temperatures. After this time, the incubations were stopped by sectioning the core in 1-cm intervals to 5 cm depth and in two centimeter intervals below this depth to the bottom of the core. Sediment sections were transferred into 50 mL plastic centrifuge tubes containing 20 mL zinc acetate (20% v/v) and shaken vigorously and frozen. The total amount of ^{35}S-labeled reduced sulfur (TRIS) was determined using the single-step cold distillation method by Kallmeyer et al. (2004). TRIS and supernatant sulfate were counted on a TriCarb 2095 Perkin Elmer scintillation counter. The sulfate reduction rate was calculated using the following equation (Jørgensen, 1978):

$$^{35}SRR = \left(TRI^{35}S \Big/ (^{35}SO_4^{2-} + TRI^{35}S) \right) \cdot 1.06 \cdot SO_4^{2-} \cdot \rho \cdot 1/t \qquad (2)$$

where SO_4^{2-} is the pore water sulfate concentration corrected for porosity ρ, $TRI^{35}S$ and $^{35}SO_4^{2-}$ are the measured counts (cpm) of total reduced inorganic sulfur species and sulfate, respectively, 1.06 is a correction factor accounting for the isotope discrimination of ^{35}S against ^{32}S-sulfate, and t is the incubation time. The sulfate reduction rate is reported as nmol cm^{-3} day^{-1}. Generally, when cores were available ^{35}SRR were measured on replicate cores for all depth intervals. The detection limit of the rate measurements accounting for distillation blanks and radioactive decay of ^{35}S between experiment and laboratory workup was 0.1 nmol day^{-1} cm^{-3}.

2.7 Whole-core sediment incubations

Four intact cores with undisturbed sediment surfaces and clear overlying water were subsampled in the laboratory in acrylic tubes (i.d. 6.2 cm, height 25 cm) retaining about 10

cm of the overlying water. The sediment height in the tubes was approximately 10 cm. The cores were incubated in a 40 L incubation tank filled with bottom water from the same station. Before the incubation the overlying water in the cores was equilibrated with bottom water in the tank. The overlying water in the cores was stirred by small magnetic bars mounted in the core liners and driven by an external magnet at 60 rpm. The cores were pre-incubated uncapped for 6 hours and subsequently capped and incubated for a period of 6 to 12 hours depending on the initial oxygen concentration in the bottom water.

2.8 Total oxygen uptake

Oxygen sensor spots (Firesting oxygen optode, PyroScience GmbH, Germany) with a sensing surface of a diameter of 5 mm were attached to the inner wall of two incubation cores (diameter 5.5 cm). The sensor spots were calibrated against O_2-saturated bottom water and oxygen-free water following the manufacturer's guidelines accounting for temperature and salinity of the incubation water. Measurements were performed with a fiberoptic cable connected to a spot adapter fixed at the outer core liner wall at the spot position. The O_2 concentration was continuously logged during incubations. Sediment total oxygen uptake (TOU) rates were computed by linear regression of the O_2 concentration over time.

2.9 Methane fluxes

Methane fluxes were determined from discrete water samples collected in 12 mL Exetainers (Labco, Wycombe, UK) prefilled with 50 µL of 50% $ZnCl_2$ without headspace. Samples were collected at the beginning (time zero) and at the end of the incubation (time final), usually after 24 hours. CH_4 concentrations were determined using the headspace equilibration

technique (Kampbell et al., 1989) by replacing 3 mL of the water in the exetainers with high-purity helium gas at atmospheric pressure. The Exetainers were then shaken at 400rpm on a shaking table for 60 minutes to allow the gas to equilibrate between the headspace and the liquid phase and left to rest for half an hour. After equilibration 2.5 mL of NaCl brine was injected into an Exetainer to push the gas samples into an injection syringe while maintaining the headspace pressure. The samples were injected onto a 1 mL injection loop of a gas chromatograph (SRI 8610C) with FID detector using N_2 as carrier gas. CH_4 standards 5 ppm, 100 ppm and 1000 ppm (Air Liquide) were used to construct a calibration curve. The partial pressure of CH_4 in the equilibrated headspace and water was calculated using the solubility coefficient β for CH_4 (Wilhelm et al 1977), gas constant R (8.314 L kPa mol^{-1} K^{-1}), air pressure P (kPa), headspace gas concentration $CH_{4\ hsp}$ (nmol), headspace volume (0.003 L), water volume in the exetainer (0.009 L), and laboratory temperature T (293 K) according to

$$CH_4\ (nM) = (CH_{4\ hsp} + \beta\ CH_{4\ hsp})^* P/RT \quad (3)$$

Fluxes (J) of CH_4 (mmol m^{-2} d^{-1}) during the whole core sediment incubations were calculated according to

$$J = (CH_{4\ start} - CH_{4\ end})/t * V/A \quad (4)$$

where $CH_{4\ start}$ and $CH_{4\ final}$ represent the end and start concentrations in mmol/m^3, V is headspace volume (m^3), A is the surface area of the incubation core (m^2), and t is the incubation time (days).

2.10 Diffusive flux calculations

Diffusive fluxes of methane and sulfate were estimated from the porewater gradients of methane and sulfate for the sediment surface and the sulfate-methane transition zone.

Sediment cores at station B1 showed occasional burrows from deposit feeders in the topmost 2 cm of sediment, whereas sediment at station H6 was largely devoid of macro- and meiofauna. Since only one sample was taken from the topmost 2 cm, quantitative depth-related effects of bioturbation cannot be accounted for in this analysis and upward diffusive transport of methane was assumed as the dominant transport pathway. Fluxes were estimated using Fick's first law of diffusion

$$J = D_s \frac{dC}{dx} \quad (5)$$

assuming that flux was dominated by molecular diffusion, where dC is the change in concentration of dissolved sulfate (mM) or methane (mM) over a depth interval dx (cm), and D_s is the sediment diffusion coefficient corrected for temperature and salinity according to Boudreau (1996). D_s was recalculated from the molecular diffusion coefficient D_o for sulfate and methane according to Iversen and Jørgensen (1994).

3 Results

3.1 Bottom water temperature, dissolved oxygen, organic carbon

Over the observation period April 2012 through February 2013 bottom water salinity varied between 6.5 and 7.0‰ at station B1 and 5.4 and 6.5‰ at station H6 (Table 1), while bottom water temperatures ranged from 2.4°C to 6.9°C for station B1 and 1.8°C to 9.4°C for station H6. The lowest and highest bottom water oxygen concentrations measured were 160 µM for station B1 and 40 µM for station H6 in April 2012, and 300 µM and 380 µM for station B1 and station H6 in February 2013, respectively. Surface sediment organic carbon concentrations were similar at the two stations ranging between 4.6 % and 5.2 % at station B1, and 5.0 % and 6.0 % at station H6 over the observation period.

293 **3.2 Methane and sulfate concentrations**

294 The highest methane concentrations in the sediment cores were recorded in October 2012 at
295 station B1, when they reached 1.9 mM, and August 2012 at station H6, when they reached 5.7
296 mM (Figure 2 a-h). Methane concentrations were lowest in February, when the highest
297 concentrations in the cored sediment were only 0.1 mM at station B1 and 1.5 mM at station
298 H6. The measured methane concentrations never exceeded the solubility limit for methane
299 calculated for the *in situ* pressure, which ranged from 9.6 to 11.9 mM during the different
300 sampling periods. Generally, methane concentrations at station H6 increased linearly from the
301 surface down to 10 cm depth. Below this depth they only increased slightly or remained
302 constant. An exception to this trend was observed in February at station B1, when the
303 methane concentration profile indicated net consumption of methane in the topmost 10 cm of
304 sediment.
305 Sulfate concentration gradients changed considerably between the different seasons at both
306 stations reflecting substantial changes in sulfate reduction rates over the observation period.
307 At both stations, the sulfate concentration gradients were steepest in October, intermediate in
308 April and August, and lowest in February indicating highest and lowest sulfate reduction rates
309 in October and February, respectively (Figure 2 a-h). At station B1, sulfate was never
310 consumed completely and concentrations remained above 1.5 mM at the bottom of the core.
311 Generally, sulfate decreased steeply from the surface down to 10 cm depth in August and
312 October. Below this surface zone there was an interval with nearly constant concentrations
313 down to 20 cm depth, below which sulfate decreased again to a concentration to about 1.5
314 mM. Despite some variability in the sulfate concentration profiles and a lower gradient in the
315 topmost centimeters in April and February, the sulfate concentrations at the bottom of the core
316 were similar during all observation periods. At station H6, sulfate was always depleted in the
317 cored sediment interval, albeit at substantially greater depth in February. Depletion already

318 occurred at 5 cm depth in April and October and at 9 cm depth in August, and sulfate
319 concentrations showed a typical concave gradient.
320
321 **3.3 ^{35}S-sulfate reduction rates**
322 At station B1, depth-integrated sulfate reduction rates over the core length varied from 0.5 to
323 2.3 mmol m^2 d^{-1} and SRR ranged from 63 nmol cm^{-3} d^{-1} at the sediment surface to 0.2 nmol
324 cm^{-3} d^{-1} at the bottom of the cored intervals (Figure 3 a-h, Table 2). The highest SRR were
325 measured in the topmost 2 cm with the exception of October 2012, when the maximum was
326 found at 3 cm depth. Below the maximum, rates decreased exponentially indicating that
327 organoclastic sulfate reduction dominated and that the reactivity of the degrading organic
328 material decreased exponentially with depth. Over the cored sediment interval, there was no
329 second peak that could be attributed to significant AOM. Nevertheless, the distinct curvature
330 of the methane concentration profile in February 2013 at station B1 indicates that methane
331 was oxidized in the sulfate reduction zone and that some sulfate reduction was coupled to
332 anaerobic methane oxidation. Organiclastic sulfate reduction and anaerobic methane
333 oxidation co-occurred in these depth intervals. Overall, no clear seasonal trend was found in
334 the rates and winter rates were comparable to summer and fall rates.
335 At station H6, the highest measured SRR was 338 nmol cm^{-3} d^{-1} and occurred at 2 cm depth in
336 April 2012. Organoclastic sulfate reduction dominated the interval down to 10 cm. Depth-
337 integrated sulfate reduction rates over the core length varied 9.2 to 11.7 mmol m^{-2} d^{-1} at station
338 H6. In April, August, and October 2012 two distinct sulfate reduction rate peaks were found
339 at station H6, one at the surface and a second peak between 10 cm and 15 cm depth. The latter
340 is in the sulfate-methane transition zone and indicates that in this depth interval the rates of
341 anaerobic methane oxidation coupled to sulfate reduction exceeded organoclastic sulfate
342 reduction rates. Previous studies at nearby station H5 in Himmerfjärden also found AOM to
343 be present at depths between 6 and 16 cm, which is in agreement with our findings (Wegener

et al., 2012). The depth-integrated rates of ^{35}SRR in the sulfate-methane transition zone at H6 were relatively constant over the three observation periods and varied between 2.4 mmol m^{-2} d^{-1} and 2.8 mmol m^2 d^{-1} (Table 2). In February, however, when sulfate penetrated to 24 cm depth, sulfate reduction rates were about two times lower compared to the other months. The previously observed deeper sulfate reduction peak between 10 and 15 cm depth was not visible, although a SRR peak was observed between 5 and 9 cm depth. However, the high concentrations of sulfate and low concentrations of methane in this depth interval in February make it unlikely that this peak is due to AOM. It is more likely that this peak is associated with organiclastic sulfate reduction, because no change in the sulfate or methane gradients was observed at this depth. Sulfate reduction was also detected below the sulfate-methane transition zone at station H6 in April, August, and October. Since non-radioactive carrier sulfate was added to the ^{35}S-tracer during these incubations, these rates indicate potential sulfate reduction activity in the methanogenic zone (Leloup et al., 2009).

3.4 Benthic exchange of oxygen, sulfate, and methane

Rates of total oxygen uptake are summarized in Table 2 and shown for comparison in Figure 4. Total oxygen uptake was lowest in February at both stations (B1: -12 ± 2.5 mmol m^{-2} d^{-1} and H6: -14.9 ± 3.5 mmol m^{-2} d^{-1}), and highest in April at station B1 (-33.5 ± 4.7 mmol m^{-2} d^{-1}) and in August at station H6 (-26.9 ± 3.7 mmol m^{-2} d^{-1}). Diffusive fluxes of sulfate from the water column into the sediment ranged from -0.2 mmol m^{-2} d^{-1} in February to -1.4 mmol m^{-2} d^{-1} in October at station B1, and from -1.3 mmol m^{-2} d^{-1} in February to -2.7 mmol m^{-2} d^{-1} in August at station H6 (Table 2). These rates are significantly lower than the radiotracer rates and indicate that sulfate is reoxidized below the sediment surface by reaction with reactive iron (Thang et al., 2013). Whole-core methane fluxes ranged from 0.1 mmol m^{-2} d^{-1} (February and April) to 1.2 mmol m^{-2} d^{-1} (August) at station B1 and from 10.3 mmol m^{-2} d^{-1} (February)

to 19.9 mmol m^{-2} d^{-1} (August) at station H6 (Figure 4, Table 2). Diffusive methane fluxes ranged from 0.05 mmol m^{-2} d^{-1} to 1.6 mmol m^{-2} d^{-1} at station B1 and from 0.4 to 2.6 mmol m^{-2} d^{-1} in August at H6. Methane fluxes determined by whole-core incubation and fluxes determined from the concentration profiles of dissolved methane gave similar results at station B1, but whole-core incubation fluxes were consistently higher at station H6 (Table 2), but the general seasonal variability in fluxes at the two stations was similar with the two measuring methods (Table 2). The very high value measured in August 2012 at station H6 is likely due to ebullition during the incubation at ambient air pressure. The good agreement between whole-core fluxes and diffusion-based fluxes at station B1 suggests that bioturbation and irrigation at this station had little influence on the methane exchange with the bottom water.

4 Discussion

4.1 Bottom water temperature and salinity

Correlations between biogeochemical rates and fluxes with bottom water temperatures in Himmerfjärden between April 2012 and February 2013 were weak for the period April-October, and forced by the low rates in the coldest observation period in early February 2013. The temperature versus rate/flux relationships were generally non-linear and not consistent for the fluxes of oxygen, methane, and sulfate indicating that additional controlling factors played a role. It is likely that the microbial community involved in the cycling of methane and sulfur species in Himmerfjärden sediment is temperature-sensitive, and that the low rates in February 2013 are due to the 3°C temperature drop in bottom water from October 2012 to February 2013. This would be consistent with rate observations in comparable environments by Treude et al (2005a), Abril and Iversen (2002), Crill and Martens (1983), and Westrich and Berner (1988), and is also supported by studies of the microbial community composition of

394 estuarine sediments that showed variations as a function of temperature (e.g., Zhang et al
395 2014). Regulation of methane fluxes largely by temperature implies that methane oxidation in
396 Himmerfjärden sediment is less temperature-sensitive than methanogenesis preventing
397 methane oxidizers from keeping up with the enhanced methane flux during summer. This
398 requires significantly higher temperature stimulation of methanogens than methane oxidizers
399 or lack of an electron acceptor for methane oxidation. Publications from lake environments
400 and terrestrial environments suggest that aerobic methane-oxidizing bacteria may indeed be
401 less temperature-sensitive than methanogens (King, 1992; Wik et al., 2014; Nguyen et al.,
402 2011). However, this argument is not well supported for marine habitats. In case of anaerobic
403 methane oxidation, it is difficult to argue for a physiological temperature disadvantage of
404 methane oxidizers compared to methanogens, because of the tight coupling between sulfate
405 reduction and methane oxidation, the phylogenetic proximity of ANME to known
406 methanogenic Archaea (Knittel and Boetius, 2009), and similarities in membrane composition
407 of ANME and methanogenic Archaea (Wegener et al., 2012). Further, microbial community
408 composition and biogeochemical rates often cannot be directly established from binary
409 relationships with temperature, since other physical and chemical parameters such as salinity,
410 bottom water oxygen concentrations, organic carbon accumulation also vary seasonally. Of
411 these, salinity is not considered to be important for the present study, because the annual
412 variation in Himmerfjärden bottom water was only between 5.4 and 7 ‰, which is too small
413 to affect the major electron acceptor and carbon degradation pathways.
414
415 **4.2 Effects of organic matter composition and sedimentation**
416 Organic carbon concentrations in Himmerfjärden are comparable to other fjord- and fjärd-
417 type estuarine sediments (Bianchi, 2007; Smith et al., 2015). Primary organic carbon export in
418 Himmerfjärden varies strongly on both seasonal and interannual timescales. The major export

periods occur during the spring phytoplankton bloom in March-April to early May, a late-summer cyanobacterial bloom in August, and a secondary phytoplankton bloom in September (Bianchi et al., 2002; Zakrisson et al., 2014; Harvey et al., 2015). Terrestrial-derived organic carbon that is not derived from the sewage treatment plant plays only a minor role in this system, because no major rivers enter the system and surface rainwater runoff is low. Based on sediment trap studies, the annual organic carbon flux in Himmerfjärden varies by more than an order of magnitude at station B1 and by about a factor of 3 in the inner parts of Himmerfjärden (Blomqvist and Larsson, 1994). However, only 10% to 60% of the total vertical mass flux may be composed of primary organic carbon, while the remainder has been interpreted as resuspended material (Blomqvist and Larsson, 1994).

A second effect to be considered is that stations B1 and H6 are located in bathymetric depressions. H6 is in the center of a sub-basin separated from the outer Himmerfjärd by a sill (Fig. 1). Likewise, station B1 is located in a small depression at the head of a submarine channel that opens to the Baltic Sea. Fine-grained and reworked organic-rich material preferentially accumulates in these depressions (Jonsson et al., 2003). Because of the importance of resuspended organic material for the vertical mass flux and bioturbation, the annual variability in the organic matter composition at the sediment surface varies year-round only between 5 % and 6 % OC with relatively constant C/N ratios between 7.9 and 9.1 at station B1 and 8.3 and 9.2 at station H6 (Bonaglia et al., 2014). Organic mass accumulation rates in the accumulation bottoms based on ^{210}Pb dating are reported to be between 3.3 and 9.5 mol m^{-2} d^{-1} (Karlsson et al., 2010; Thang et al., 2013;). The combined effect of the sedimentation characteristics is that temporal variability in the settling primary organic carbon flux above the sediment surface is low, which reduces the overall temporal variability in organic carbon amount and composition and thereby in carbon mineralization rates. This small temporal variability is further influenced by macrofauna bioturbation in the top 5 cm of

sediment in this area, foremost by the bivalve *Macoma baltica*, the arthropod *Pontoporeia femorata*, and the polychaete *Marenzelleria* (Bonaglia et al., 2014). Although macrofauna is largely absent at station H6, sediment is also mixed at station H6 by bioturbating meiofauna (mostly ostracods) (Bonaglia et al., 2014).

The measured benthic oxygen uptake rates are consistent with the low variability in the surface organic carbon concentrations, C/N ratios, and a temperature-dependent decrease in total oxygen uptake rates in winter. The slightly higher total oxygen uptake rate at station H6 is also consistent with the physiography of the enclosed small basin favouring sediment trapping of fine material. In addition, the location of station H6 in the inner fjärd limits water exchange and leads to greater oxygen depletion, whereas the more open station B1 is affected by upwelling of oxygen-rich waters and comparatively less burial of organic material (Table 1).

4.3 Methane fluxes, sulfate reduction and methane oxidation

Sediment focusing in the sub-basins of the inner Himmerfjärden sediments results in very high sedimentation rates between 0.9 and 1.3 cm/yr (Thang et al., 2013; Bianchi et al., 2002). In such sediments organic carbon burial and transfer of organic matter into the methanogenic zone is efficient and will occur within 20 to 30 years. As a consequence of the low bottom water salinity of 6 ‰ of the Baltic Sea at this latitude, seawater sulfate concentrations are less than 7 mM and, by comparison with normal seawater, a comparatively lesser amount of organic matter can be degraded by bacterial sulfate reduction (Thang et al., 2013). Consequently, compared to normal marine sediments a larger proportion of organic matter undergoes anaerobic microbial degradation terminating in methanogenesis, which generates a high upward flux of methane into the sulfate-containing zone. Organiclastic sulfate-reducing bacteria will compete for the available sulfate with sulfate-reducing bacteria involved in the

anaerobic oxidation of methane (Dale et al., 2006; Jørgensen and Parkes, 2010). Thermodynamic and kinetic constraints decide on the result of this competition between these two processes. Dale et al. (2006) suggested that due to lower winter temperatures and greater sulfate availability in the sulfate-methane transition zone in winter, the thermodynamic driving force for anaerobic methane oxidation increases allowing for a greater proportion of anaerobic methane oxidation coupled to sulfate reduction in the winter. In the summer and fall, higher temperatures and sulfate limitation favor organiclastic sulfate reduction and methanogenesis while limiting the anaerobic oxidation of methane. Most importantly, however, their analysis showed that due to thermodynamic constraints and slow growth rates of the methane-oxidizing archaea the microbial biomass does not change significantly over a year. These conceptual modelling results can be tested with our Himmerfjärden data.

Sulfate reduction rates, particularly at H6, demonstrate how strongly bottom-water oxygen controls organic matter mineralization. In the spring, summer, and fall sulfate reduction was at its maximum in the first two centimeters of the sediments (Fig 3 e, f, g). In February, reduced organic carbon input and higher oxygen concentrations resulted in lower sulfate reduction rates and a shift of the maximum rates to greater depths in the sediment (Figure 3 h). Since other terminal carbon-oxidizing processes (e.g. denitrification, iron, and manganese reduction) outcompete sulfate reduction for electron-donating substrates, the depth of sulfate penetration and organic matter degradation via sulfate shifts deeper in the sediment, which reduces methane production.

The decrease in oxygen uptake matches well with the decrease in methane fluxes at the two stations in winter, which suggests an impact of oxygen on methane cycling (Table 2, Figure 4). Higher oxygen levels enhance bioturbation and oxygen uptake by the abundant macro- and meiofauna (Norkko et al., 2015), but the mixing of sediment also affects methane transport to the water column, as the main transport process shifts from diffusion to advection. This effect

494 is likely the main cause for the winter decrease in methane fluxes and concentrations. More
495 aerated conditions indirectly enhance methane removal by sustaining aerobic methanotrophs
496 (Valentine 2011). It is plausible that, as in other brackish coastal sediments, aerobic
497 methanotrophs at the surface of Himmerfjärden sediments consume a significant part of
498 upward-diffusing methane that was not oxidized by anaerobic methane oxidation (McDonald
499 et al 2005, Moussard et al 2009, Treude et al 2005a).
500 Published benthic methane fluxes for estuaries with similar salinities have a reported range of
501 0.002 to 0.25 mmol m^{-2} d^{-1} (Abril and Iversen, 2002; Martens and Klump, 1980; Sansone et
502 al., 1998; Zhang et al., 2008; Borges and April, 2012; Martens et al., 1998). The methane
503 fluxes derived from our core incubations (0.1-2.6 mmol m^{-2} d^{-1}, ignoring the potentially
504 biased value of 19.9 mmol m^{-2} d^{-1}) were high compared to these published fluxes. Our fluxes
505 are consistent with fluxes based on porewater gradients by Thang et al. (2013) that were
506 between 0.3 and 1.1 mmol m^{-2} d^{-1} at 3 nearby stations measured in May 2009.
507 A conspicuous property of all porewater profiles at station H6, with the exception of the
508 February 2013 sampling period, was the absence of a curvature in the methane concentration
509 profiles, which would be expected for net methane oxidation by aerobic and anaerobic
510 methane oxidation (Martens et al., 1998). Most concentration profiles of sulfate and methane
511 at station H6 overlapped without a significant change in the methane concentration gradient.
512 A similar observation has been made earlier for other Himmerfjärden sediments (Thang et al.,
513 2013), and has also been reported for sediments of the northwestern Black Sea shelf (Knab et
514 al., 2009) and in organic-rich shelf sediment of the Namibian upwelling system (Brüchert et
515 al., 2009). Inefficient methane oxidation is also evident from the diffusive fluxes, which
516 showed that the upward fluxes of methane into the sulfate-methane transition zone were only
517 marginally higher than the methane fluxes to the sediment surface indicating little attenuation
518 of the methane flux in the sulfate-methane transition zone (Table 2). One possible explanation

519 for this phenomenon is therefore that rates of sulfate reduction–coupled anaerobic methane
520 oxidation, except for the winter months, were low compared to the total sulfate reduction rate.
521 An alternative explanation of our observations could be that the methane concentration
522 gradients were affected by the presence of rising methane bubbles (Haeckel et al., 2007), or
523 that bioturbation and bioirrigation linearized the concentration profiles (Dale et al., 2013).
524 However, we do not favor this interpretation because of the absence of large macrofauna at
525 station H6, the fact that methane concentrations were below the in-situ saturation
526 concentration of methane, and the fast porewater methane sampling method.
527 An analysis of the cumulative distribution of ^{35}S-SRR with depth at station H6 provides clues
528 to the proportion of organoclastic relative to anaerobic methane oxidation-coupled sulfate
529 reduction at station H6 (Figure 5 e-h). The gradient in organoclastic sulfate reduction is well
530 described by the exponential function,
531 $$^{35}SRR = a\ z^{-b} \quad (6)$$
532 where z is depth (cm) and a and b are regression coefficients (Jørgensen and Parkes, 2010).
533 For the sediments investigated here, the exponential coefficient b varied between 0.4 and 0.9
534 at station B1 and 0.3 and 0.8 at station H6 (Table 3). At station H6 the lowest coefficient was
535 found for February 2013, when sulfate penetrated the deepest into the sediment. Since the
536 upward flux of methane provides an additional energy source to sulfate-reducing bacteria,
537 sulfate reduction rates are expected to increase in the sulfate-methane transition zone. If
538 substantial AOM-coupled and organiclastic sulfate reduction occur at the same depths the
539 total ^{35}S-sulfate reduction rate depth gradient will be lower and the exponential coefficient b
540 will be smaller than for a setting without AOM. The difference between the exponential
541 coefficients for the different observation times can be used to calculate the variation in the
542 contribution of AOM to the total sulfate reduction rate. At station H6, between 5 % (August
543 2012) and 20% (April 2012) of the total sulfate reduction can be associated with anaerobic

544 methane oxidation. A comparison of the above method with the ^{35}S-sulfate reduction rates
545 integrated over the length of the H6 sediment cores with the rates integrated in the AOM zone
546 also indicated that >20% of sulfate reduction at H6 was supported by anaerobic methane
547 oxidation (Table 2). In near-shore continental margin sediments worldwide, the fraction of
548 methane-driven sulfate reduction varies between locations and accounts for 3-40% of total
549 sulfate reduction, with 10% possibly representing a global mean value (Jørgensen and Kasten,
550 2006). The average 20% contribution calculated here falls in the upper range of these values
551 and is similar to values reported before for one of the monitoring stations within
552 Himmerfjärden (Thang et al., 2013) and also for a very productive Chilean slope sediment (8-
553 24 %) (Treude et al 2005b). The good match between the upward fluxes of methane in the
554 sulfate-methane transition zone and the measured sulfate reduction rates in the transition zone
555 also indicate that other proposed electron acceptors for anaerobic methane oxidation such as
556 iron are unimportant in these sediments (Beal et al., 2009; Egger et al. 2014).
557
558 **4.4 Temporal variability in hydrostatic pressure**
559 The abrupt decrease in porewater methane concentrations from November 2012 to late
560 January/early February 2013 and the subsequent increase in April 2013 cannot be explained
561 by variation in methane oxidation alone, because the temporal change in porewater methane
562 concentration was large compared to the inferred methane oxidation rates based on fluxes in
563 and out of the AOM zone. In addition, except for downward-diffusing sulfate, there was no
564 significant other electron acceptor present at depth. It is unlikely that rates of methanogenesis
565 would have decreased significantly between the fall and the winter and resumed again in the
566 spring because of the sedimentological characteristics described above and the small
567 difference in sediment temperatures for February and April (Table 1). Changes in organic
568 matter sedimentation at the sediment surface also have no significant influence on

569 methanogenesis in buried sediment and cannot explain the sudden decrease in methane
570 concentration at depth. An alternative explanation for the changes in methane concentrations
571 is required. A possible explanation could be that changes in upward transport of methane are
572 due to variability in hydrostatic pressure and the associated diffusive and advective upward
573 transport of methane from depth. The free gas depth of methane is thought to follow changes
574 in hydrostatic pressure and temperature (Mogollon et al., 2011; Toth et al., 2015). An
575 estimated 10% of the fine-grained sediments in the Stockholm archipelago area are underlain
576 by pockets of free methane (Persson and Jonsson, 2000) and these free gas pockets are
577 preferentially located in areas with the thickest postglacial mud accumulation, generally in the
578 center of the sub-basins and along fault lineaments (Söderberg and Floden, 1992). Based on
579 sub-bottom echosounder profiling, the surface of the free gas zone in accumulation areas in
580 Himmerfjärden and other areas of the Stockholm archipelago is between 1 and 3 meter depth
581 (Söderberg and Floden, 1991). During low sealevel stand the free gas zone is expected to
582 migrate closer to the sediment surface, whereas during high sealevel the free gas zone is
583 depressed into the sediment. The total variation in sealevel is related to air pressure,
584 prevailing wind directions, precipitation, the balance of saltwater entry through the Danish
585 straits, and freshwater discharge from rivers entering the Baltic Sea (Andersson, 2002).
586 Additional effects are caused by local coastal bathymetry, current flow, and, possibly, local
587 submarine groundwater discharge. These multiple parameters result in complex subsurface
588 hydrology and may produce sealevel fluctuations that can be as much as 50 cm, sufficient to
589 explain the changes in methane concentrations observed here. Unfortunately, local data within
590 Himmerfjärden on sealevel fluctuations are not available for our respective sampling
591 locations, and regional sealevel stands should not be directly applied to the sample sites. The
592 above discussion demonstrates that a variety of processes interact in these fjord sediments to
593 produce the observed methane fluxes. It is beyond the scope of this paper to develop a

unifying model against which the variability of the observed fluxes can be tested, but we would like to point out that the local coastal hydrography and hydrogeology would need to be accounted for in such a coupled physical biogeochemical model. To our knowledge, sufficient subsurface geophysical data are currently not available to establish appropriate physical boundary conditions for such a model. Detailed geophysical analysis of the subsurface structure at high vertical resolution together with long-term monitoring of the porewater chemistry would shed new light on the coupling between subsurface hydrology and methane emissions.

5 Conclusions

A greater understanding of methane emissions from estuarine and coastal sediments is important to estimate the contribution of these environments to global marine methane fluxes. High benthic fluxes of methane from these sediments showed that total methane oxidation was relatively inefficient, despite the fact that anaerobic methane oxidation contributed up to 20% to total sulfate reduction. Higher bottom water oxygen concentrations in winter played an important role in methane removal in these sediments. Of the different environmental regulators, bottom water oxygen had the strongest influence on the regulation of methane emissions. Oxygen availability directly enhanced aerobic organic matter mineralization by shifting the redox cascade in the sediments and indirectly by stimulating meiofauna and macrofauna activity thereby stimulating both the aerobic carbon mineralization and oxidative recycling of sulfate. The annual variability in sediment methane concentrations and benthic methane fluxes indicate that the annual environmental changes at these near-shore, but relatively deep-water localities are considerable. Very few data on sediment biogeochemical processes are currently available for aerobic and anaerobic carbon mineralization and methane cycling during winter months when ice cover inhibits access and sampling. Process rates

619 inferred from sampling during open-water conditions over the whole year are therefore likely
620 overestimates. Hydrostatic pressure changes and complex subsurface hydrological conditions
621 may also affect the temporal variability of subsurface methane concentrations. The spatial and
622 temporal variability of these conditions must also be considered as an important component
623 for understanding methane emissions from near-shore coastal and estuarine waters.
624
625

6. Author contribution

Volker Brüchert devised the study, interpreted the data, created the figures and tables, wrote and revised the manuscript. Joanna E. Sawicka conducted the sampling and analysis for the study and contributed to the writing.

7. Data availability

The data are available from the second author upon request.

8. Acknowledgments

We are grateful to the staff of Askö Laboratory for their help and cooperation during the cruises and our stays at Askö laboratory. We would like to thank Barbara Deutsch, Camilla Olsson and Stefano Bonaglia for their help during sampling. The study was funded by the grant from the Bolin Centre for Climate Research, Baltic Ecosystem Adaptive management (BEAM), and the EU BONUS+ project Baltic Gas.

References

Abril, G. and Iversen, N.: Methane dynamics in a shallow non-tidal estuary (Randers Fjord, Denmark), Mar Ecol Prog Ser, 230, 171-181, 2002.

Amouroux, D., Roberts, G., Rapsomanikis, S. and Andreae, M.O.: Biogenic gas (CH_4, N_2O, DMS) emission to the atmosphere from near-shore and shelf waters of the North-western Black Sea, Estuar Coast Shelf S, 54, 575-587, 2002.

Andersson, H.C.: Influence of long-term regional and large-scale atmospheric circulation on the Baltic sea level, Tellus A 54, 76-88, 2002.

Bange, H. W., Bergmann, K, Hansen, H. P., Kock, A., Koppe, R., Malien, F., Ostrau, F., Dissolved methane during hypoxic events at the Boknis Eck time series station (Eckernförde Bay, SW Baltic Sea), Biogeosciences, 7, 1279-1284, 2010.

Beal, E. J., House, C. H., Orphan, V. J.: Manganese- and Iron-Dependent Marine Methane Oxidation, Science 325, 184-187, 2009.

Bianchi, T. S., Engelhaupt, E., McKee B. A., Miles, S., Elmgren, R., Hajdu, S., Savage, C., and Baskaran, M.: Do sediments from coastal sites accurately reflect time trends in water column phytoplankton? A test from Himmerfjärden Bay (Baltic Sea proper), Limnol. Oceanogr., 47, 1537-1544, 2002.

Blomqvist, S. and Larsson, U.: Detrital bedrock elements as tracers of settling resuspended particulate matter in a coastal area of the Baltic Sea, Limnol. Oceanogr., 39, 880-896, 1994.

Boesch, D. F., Hecky, R., O'Melia, C., Schindler, D., Seitzinger, S.: Eutrophication of the Swedish Seas, Reports of the Swedish Environmental Protection Agency, Stockholm, Sweden, No. 5509, 72 p, 2006.

Bonaglia, S., Bartoli, M., Gunnarsson, J. S., Rahm, L., Raymond, C., Svensson, O., Shakeri, Brüchert, V.: Effect of reoxygenation and Marenzelleria spp. bioturbation on Baltic Sea sediment metabolism, Marine Ecology Progress Series, 482, 43-55, 2013.

Bonaglia, S., Deutsch, B., Bartoli, M., Marchant, H. K. and Brüchert, V.: Seasonal oxygen, nitrogen and phosphorus benthic cycling along an impacted Baltic Sea estuary: regulation and spatial patterns, Biogeochemistry, 119, 1-22, 2014.

Borges, A. V. and Abril, G.: Carbon Dioxide and Methane Dynamics in Estuaries, in: Treatise on Estuarine and Coastal Science, (Eds.) Wolanski, E., McLusky, D., Academic Press, Waltham, 119-161, 2011.

Boudreau, B.P.: Diagenetic models and their implementation. Springer Verlag, Berlin Heidelberg, 1996.

Brüchert, V., Currie, B., Peard, K.: Hydrogen sulphide and methane emissions on the central Namibian shelf, Progr. Oceanogr., 83, 169-179, 2009.

Crill, P. M. and Martens, C. S.: Spatial and temporal fluctuations of methane production in anoxic coastal marine sediments, Limnol. Oceanogr., 6, 1117-1130, 1983.

Dale, A. W., Regnier, P., Van Cappellen, P.: Bioenergetic Controls on Anaerobic Oxidation of Methane (AOM) in Coastal Marine Sediments: A Theoretical Analysis, Am. J. Sci., 306, 246-294, 2006.

Dale, A. W., Aguilera, D. R., Regnier, P., Fossing, H., Knab, N. J., Jørgensen, B. B.: Seasonal dynamics of the depth and rate of anaerobic oxidation of methane in Aarhus Bay (Denmark) sediments, J. Mar. Res., 66, 127-155, 2008.

Dale, A. W., Bertics, V. J., Treude, T., Sommer, S., Wallmann, K.: Modeling benthic–pelagic nutrient exchange processes and porewater distributions in a seasonally hypoxic sediment: evidence for massive phosphate release by Beggiatoa? Biogeosciences, 10, 629-651, 2013.

Egger, M., Rasigraf, O., Sapart, C. J., Jilbert, T., Jetten, M. S. M., Röckmann, T.: Iron-mediated anaerobic oxidation of methane in brackish coastal sediments, Env. Sci. Technol., 49, 277-283, 2014.

Elmgren, R. and Larsson, U.: Himmerfjärden: förändringar i ett näringsbelastat kustekosystem i Östersjön, Reports of the Swedish Environmental Protection Agency, Stockholm, Sweden, 1997.

Engqvist, A., Long-term nutrient balances in the eutrophication of the Himmerfjärden, Estuar. Coast. Shelf S., 42, 483-507, 1996.

Giuseppe Etiope, G., Lassey, K.R., Klusman, R.W., Boschi, E.: Reappraisal of the Fossil Methane Budget and Related Emission from Geologic Sources, Geophys. Res. Lett., 35, ISSN 1944-8007, 2008.

Haeckel, M., Boudreau, B. P., Wallmann, K.: Bubble-induced porewater mixing: A 3-D model for deep porewater irrigation, Geochim Cosmochim, Acta, 71, 5135-5154, 2007.

693 Harvey, E. T., Kratzer, S., Philipson, P.: Satellite-based water quality monitoring for improved spatial and
694 temporal retrieval of chlorophyll-a in coastal waters, Remote Sens. Environ., 158, 417-430, 2015.
695 Iversen, N., Jørgensen, B. B.: Diffusion coefficients of sulfate and methane in marine sediments: Influence of
696 porosity, Geochim. Cosmochim. Acta 57, 571-578, 1994.
697 Jørgensen, B. B. and Kasten, S.: Sulfur Cycling and Methane Oxidation, In: Marine Geochemistry, (Eds.) Schulz
698 H. and Zabel, M., Springer, Berlin Heidelberg, 271-309, 2006.
699 Jørgensen, B. B.: A comparison of methods for the quantification of bacterial sulfate reduction in coastal marine
700 sediments, Geomicrobiol. J., 1, 11-27, 1978.
701 Jørgensen, B. B. and Parkes, R. J.: Role of sulfate reduction and methane production by organic carbon
702 degradation in eutrophic fjord sediments (Limfjorden, Denmark), Limnol. Oceanogr., 55, 1338-1352,
703 2010.
704 Jonsson, P., Persson, J., Holmberg, P.: Skärgårdens bottnar, Report of the Swedish Environmental Protection
705 Agency, Stockholm, No. 5212, 114, 2003.
706 Judd, A. G.: Natural seabed gas seeps as sources of atmospheric methane, Environ. Geol., 46, 988-996, 2004.
707 Kallmeyer, J., Ferdelman, T. G., Weber, A., Fossing, H., Jørgensen, B. B.: Evaluation of a cold chromium
708 distillation procedure for recovering very small amounts of radiolabeled sulfide related to sulfate
709 reduction measurements, Limnol. Oceanogr. Meth., 2, 171-180, 2004.
710 Kampbell, D. H., Wilson, J. T., Vandegrift, S. A.: Dissolved Oxygen and Methane in Water by a GC Headspace
711 Equilibration Technique, Intern. J. Environ. An. Ch., 36, 249-257, 1989.
712 Karlsson, M., M. Malmaeus, M., Rydin, E., Jonsson, P.: Bottenundersökningar i Upplands, Stockholms,
713 Södermanlands och Östergötlands skärgårdar: 2008-2009. Svenska Miljöinstitut, B1928, 102, 2010.
714 King, G.M.: Ecological Aspects of Methane Oxidation, a Key Determinant of Global Methane Dynamics, In:
715 Advances in Microbial Ecology, 12, Marshall, K.C. (ed.), 431-468, 1992.
716 Kirschke, S., Bousquet, P., Ciais, P., Saunois, M., Canadell, J.G., Dlugokencky, E.J., Bergamaschi, P.,
717 Bergmann, D., Blake, D.R., Bruhwiler, L.: Three Decades of Global Methane Sources and Sinks, Nat.
718 Geosci., 6, 813-23, 2013.
719 Knab, N. J., Cragg, B. A., Borowski, C., Parkes, R. J., Pancost, R. and Jørgensen, B. B.: Anaerobic oxidation of
720 methane (AOM) in marine sediments from the Skagerrak (Denmark): I. Geochemical and
721 microbiological analyses. Geochim. Cosmochim. Acta, 72, 2868-2879, 2009.
722 Knittel, K. and Boetius, A.: Anaerobic Oxidation of Methane: Progress with an Unknown Process. Ann. Rev.
723 Microbiol., 63: 311-334, 2009.
724 Klump, J. V. and Martens, C. S.: Biogeochemical cycling in an organic rich coastal marine basin—II. Nutrient
725 sediment-water exchange processes. Geochim. Cosmochim. Acta, 45, 101-121, 1981.
726 Kristensen, E., Bouillon, S., Dittmar, T., Marchand, C.: Organic carbon dynamics in mangrove ecosystems: A
727 review. Aquat. Bot., 89, 201-219, 2008.
728 Larsson, U., Nyberg, U., Höglander, H., Sjösten, A., Sandberg, M., Walve, J.: Himmerfjärdens miljörapport
729 2012, Department of Ecology, Environment, and Plant Sciences, Technical Report 50, 75, 2012.
730 Leloup, J., Fossing, H., Kohls, K., Holmkvist, L., Borowski, C., Jørgensen, B. B.: Sulfate-reducing bacteria in
731 marine sediment (Aarhus Bay, Denmark): abundance and diversity related to geochemical zonation.
732 Environ. Microbiol., 11, 1278-1291, 2009.
733 Martens, C. S., Albert, D. B., Alperin, M. J.: Biogeochemical processes controlling methane in gassy coastal
734 sediments - Part 1. A model coupling organic matter flux to gas production, oxidation, and transport.
735 Cont. Shelf Res., 18, 1741-1770, 1998.
736 Martens, C. S. and Berner, R. A.: Methane production in the interstitial waters of sulfate-depleted marine
737 sediments. Science, 185, 1167-1169, 1974.
738 Martens, C. S. and Klump, J.: Biogeochemical cycling in an organic-rich coastal marine basin. 4. An organic
739 carbon budget for sediments dominated by sulfate reduction and methanogenesis. Geochim.
740 Cosmochim. Acta, 48, 1987-2004, 1984.
741 Martens, C.S. and Val Klump, J.: Biogeochemical cycling in an organic-rich coastal marine basin—I. Methane
742 sediment-water exchange processes. Geochim. Cosmochim. Acta, 44, 471-490, 1980.
743 Marty, D., Bonin, P., Michotey, V. and Bianchi, M.: Bacterial biogas production in coastal systems affected by
744 freshwater inputs. Cont. Shelf Res., 21, 2105-2115, 2001.

McDonald, I. R., Smith, K., Lidstrom, M. E.: Methanotrophic populations in estuarine sediment from Newport Bay, California, FEMS Microbiol. Lett., 250, 287-293, 2005.
Middelburg, J., Nieuwenhuize, J., Iversen, N., Høgh, N., de Wilde, H., Helder, W., Seifert, R. and Christof, O.: Methane distribution in European tidal estuaries, Biogeochemistry, 59, 95-119, 2002.
Mogollón, J. M., Dale, A. W., L'Heureux, I., Regnier, P.: Impact of seasonal temperature and pressure changes on methane gas production, dissolution, and transport in unfractured sediments, J. Geophys. Res. Biogeosci., 116, G03031, 2011.
Moussard, H., Stralis-Pavese, N., Bodrossy, L., Neufeld, J. D., Murrell, J. C.: Identification of active methylotrophic bacteria inhabiting surface sediment of a marine estuary, Environ. Microbiol. Repts., 1, 424-433, 2009.
Musenze, R.S., Werner, U., Grinham, A., Udy, J. and Yuan, Z.: Methane and nitrous oxide emissions from a subtropical estuary (the Brisbane River estuary, Australia), Sci. Total Environ., 472, 719-729, 2014.
Nguyen, T.D., Crill, P. and Bastviken, D.: Implications of temperature and sediment characteristics on methane formation and oxidation in lake sediments, Biogeochemistry 100, 185-196, 2010.
Norkko, J., Gammal, J., Hewitt, J., Josefson, A., Carstensen, J., Norkko, A.: Seafloor Ecosystem Function Relationships: In Situ Patterns of Change Across Gradients of Increasing Hypoxic Stress, Ecosystems 18, 1424-1439, 2015.
Persson, J., Jonsson, P.: Historical development of laminated sediments–an approach to detect soft sediment ecosystem changes in the Baltic Sea. Mar. Poll. Bull., 40, 122-134, 2000.
Reeburgh, W. S.: Oceanic Methane Biogeochemistry, Chem. Rev., 107, 486-513, 2007.
Reindl, A. R. and Bolałek, J.: Methane flux from sediment into near-bottom water and its variability along the Hel Peninsula—Southern Baltic, Sea, Cont. Shelf Res., 74, 88-93, 2014.
Savage, C., Leavitt, P. R., Elmgren, R.: Effects of land use, urbanization, and climate variability on coastal eutrophication in the Baltic Sea. Limnol. Oceanogr., 55, 1033-1046, 2010.
Sansone, F. J., Holmes, M. E. and Popp, B. N.: Methane stable isotopic ratios and concentrations as indicators of methane dynamics in estuaries. Global Biogeochem. Cycles, 13, 463-474, 1999.
Sansone, F. J., Rust, T. M. and Smith, S. V., 1998. Methane Distribution and Cycling in Tomales Bay, California, Estuaries, 21, 66-77.
Seeberg-Elverfeldt, J., Schlüter, M., Feseker, T., Kölling, M.: Rhizon sampling of porewaters near the sediment-water interface of aquatic systems. Limnol. Oceanogr. Meth., 3, 361-371, 2005.
Smith, R.W., Bianchi, T.S., Allison, M., Savage, C., Galy, V.: High rates of organic carbon burial in fjord sediments globally. Nature Geosci., 8, 450-453, 2015.
Söderberg, P. and Flodén, T.: Gas seepages, gas eruptions and degassing structures in the seafloor along the Strömma tectonic lineament in the crystalline Stockholm Archipelago, east Sweden. Cont. Shelf Res. 12, 1157-1171, 1992.
Stridh, S.: SYVAB Himmerfjärdsverket Miljörapport 2012, www.syvab.se/information/dokument/syvabs-miljorapporter, 53, 2012.
Thang, N., Brüchert, V., Formolo, M., Wegener, G., Ginters, L., Jørgensen, B. B., and Ferdelman, T.: The Impact of Sediment and Carbon Fluxes on the Biogeochemistry of Methane and Sulfur in Littoral Baltic Sea Sediments (Himmerfjärden, Sweden), Estuaries and Coasts, 36, 98-115, 2013.
Tóth, Z., Spiess, V., Keil, H.: Frequency dependence in seismoacoustic imaging of shallow free gas due to gas bubble resonance, J. Geophys. Res. Solid Earth, 120, 8056-8072, 2015.
Treude, T., Krüger, M., Boetius, A., Jørgensen, B. B.: Environmental control on anaerobic oxidation of methane in the gassy sediments of Eckernförde Bay (German Baltic), Limnol. Oceanogr., 50, 1771-1786, 2005a.
Treude, T., Niggemann, J., Kallmeyer, J., Wintersteller, P., Schubert, C. J., Boetius. A., and Jørgensen, B. B.: Anaerobic oxidation of methane and sulfate reduction along the Chilean continental margin, Geochim. Cosmochim. Acta, 69, 2767-2779, 2005b.
Upstill-Goddard, R. C., Barnes, J., Frost, T., Punshon, S. and Owens, N. J. P.: Methane in the southern North Sea: Low-salinity inputs, estuarine removal, and atmospheric flux, Global Biogeochem. Cycles, 14, 1205-1217, 2000.
Valentine, D.L.: Emerging Topics in Marine Methane Biogeochemistry. Annual Rev. Mar. Sci., 3, 147-171, 2011.

Wegener, G., Bausch, M., Holler, T., Thang, N. M., Prieto Mollar, X., Kellermann, M. Y., Hinrichs, K. U., and Boetius, A.: Assessing sub-seafloor microbial activity by combined stable isotope probing with deuterated water and ^{13}C-bicarbonate. Environ. Microbiol., 14, 1517-1527, 2012.

Westrich, J. T., Berner, R. A.: The role of sedimentary organic matter in bacterial sulfate reduction: The G model tested. Limnol. Oceanogr., 29, 236-249, 1984.

Wik, M., Thornton, B.F., Bastviken, D., MacIntyre, S., Varner, R.K. and Crill, P.M.: Energy input is primary controller of methane bubbling in subarctic lakes. Geophysical Research Letters 41, 555-560, 2014.

Wilhelm, E., Battino, R., and Wilcock, R. J.: Low-pressure solubility of gases in liquid water. Chem. Rev., 77, 219-262, 1977.

Zakrisson, A., and Larsson, U.: Regulation of heterocyst frequency in Baltic Sea Aphanizomenon sp., J. Plankton Res., 36, 1357-1367, 2014.

Zhang, G., Zhang, J., Liu, S., Ren, J., Xu, J. and Zhang, F.: Methane in the Changjiang (Yangtze River) estuary and its adjacent marine area: riverine input, sediment release and atmospheric fluxes. Biogeochemistry, 91, 71-84, 2008.

Zhang, W., Bougouffa, S., Wang, Y., Lee, O. O., Yang, J., Chan C. Song, X., and Qian, P.-Y.: Toward understanding the dynamics of microbial communities in an estuarine system, PLoS ONE, 9, e94449, 2014.

Table 1. Main site characteristics of the sampling stations.

Station	Sampling time	Water depth (m)	Temperature (°C)	Bottom water salinity (‰)	Bottom water Oxygen (µM)	Surface organic carbon (%)
B1 58°48'18''N 17°37'52''E	April 2012	41	2.4	6.5	160	6.0
	August 2012		6.9	7.0	260	5.2
	October 2012		6.8	7.0	224	5.1
	February 2013		3.4	7.0	380	5.0
H6 59°04'08''N 17°40'63''E	April 2012	39.5	1.8	5.9	40	4.6
	August 2012		6.7	6.4	150	5.1
	October 2012		9.4	6.5	191	5.2
	February 2013		1.8	5.4	300	4.7

824 **Table 2.** Summary of CH_4 and SO_4^{2-} fluxes, depth-integrated ^{35}SRR, and total oxygen uptake (TOU).

Station	Sampling time	Flux (mmol m^{-2} d^{-1})						
		TOU whole core incubation (n=4)	**CH_4** whole core incubation (n=4)	**CH_4** Diffusive flux out of sediment (n=1)	**CH_4** Diffusive flux into SMTZ (n=1)[2]	**SO_4^{2-}** Diffusive flux into sediment (n=1)	**^{35}S-SRR integrated over AOM[3] zone (n=3)**	**Integrated ^{35}S-SRR (n=3)**
B1	April 2012	-19.7	1.2	1.6		-0.4	no AOM zone[4]	-2.3
	August 2012	-22.5	1.2	no data		-0.8	no AOM zone[4]	-0.5
	October 2012	-21.1	1.9	1.9		-1.3	no AOM zone[4]	-2.0
	February 2013	-12.0	0.1	0.1		-0.2	no AOM zone[4]	-2.2
H6	April 2012/13	-23.5	3.9[1]	2.2	2.8	-2.6	(10-15 cm)= 2.8	-11.6
	August 2012	-26.9	19.9[5]	2.4	2.6	-2.5	(10-15 cm) = 2.8	-11.7
	October 2012	-25.9	1.8	1.8	1.9	-2.6	(10-15 cm)=2.4	-11.5
	February 2013	-14.9	1.7	0.1	0.4	-1.3	no AOM zone[4]	-9.2

825 [1] whole core incubation was performed in April 2013; Diffusive fluxes were calculated for samples collected in
826 April 2012; [2] SMTZ - sulfate methane transition zone, [3]AOM zone – zone of anaerobic oxidation of methane, [4]
827 no AOM zone means that AOM zone was probably deeper than the core length; [5] potentially elevated due to
828 depressurization/ex-solution effect during core incubation at atmospheric pressure;

829

Table 3. Best-fit regression coefficients a and b for the depth gradient of sulfate reduction rates ($^{35}SRR = az^{-b}$ (z =depth, cm)).

Station	Sampling time	Coefficient (a)	Exponential coefficient (b)
B1	April 2012	147.0	-1.4
	August 2012	11.7	-0.9
	October 2012	16.0	-0.4
	February 2013	33.5	-0.8
H6	April 2012	18.6	-0.5
	August 2012	37.4	-0.5
	October 2012	133.2	-0.8
	February 2013	25.0	-0.4

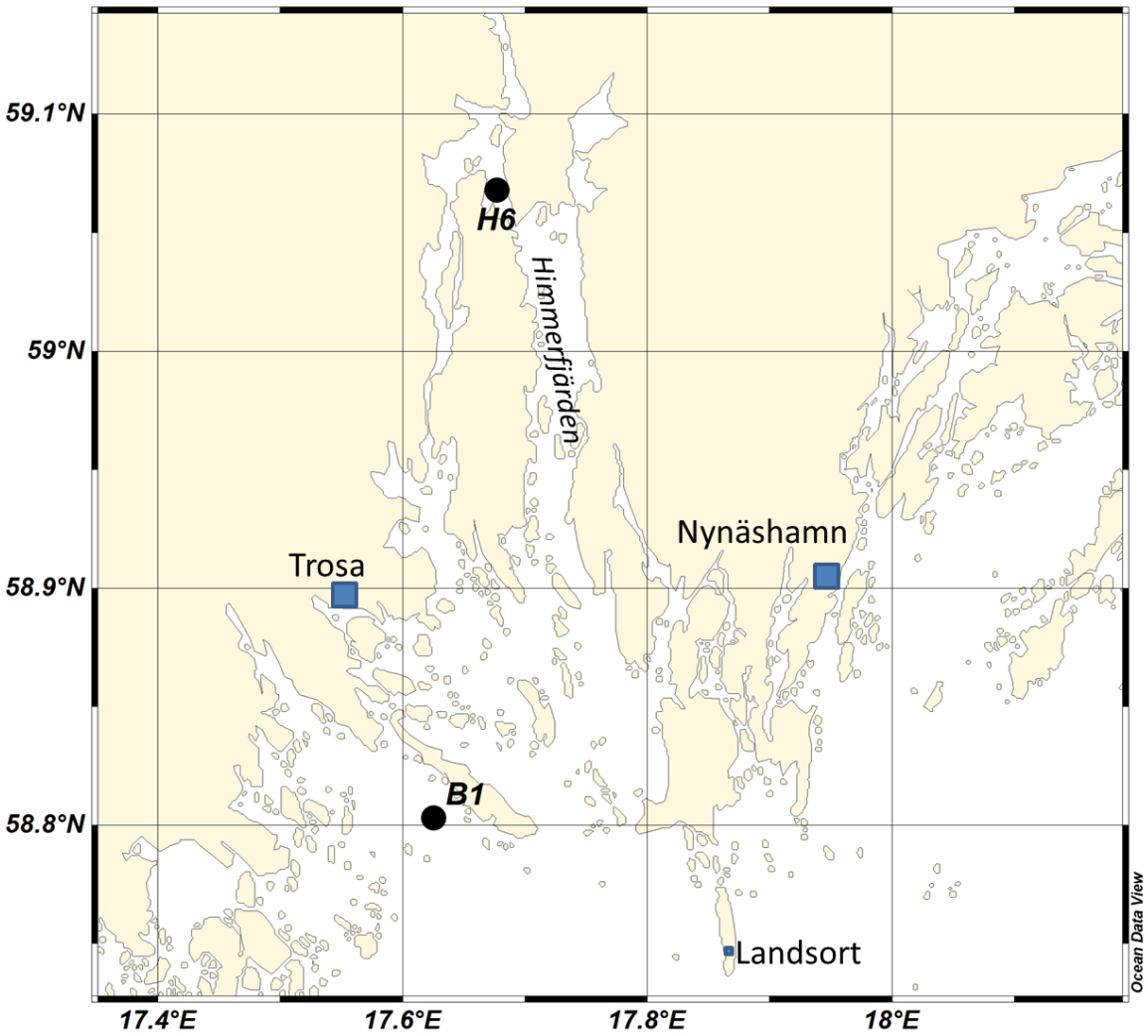

834

835

Figure 1. Location of sampling sites in Himmerfjärden, Stockholm Archipelago, Sweden. Detailed studies were conducted at two sites, an open water site (station B1) and in the inner part of the estuary (station H6).

836

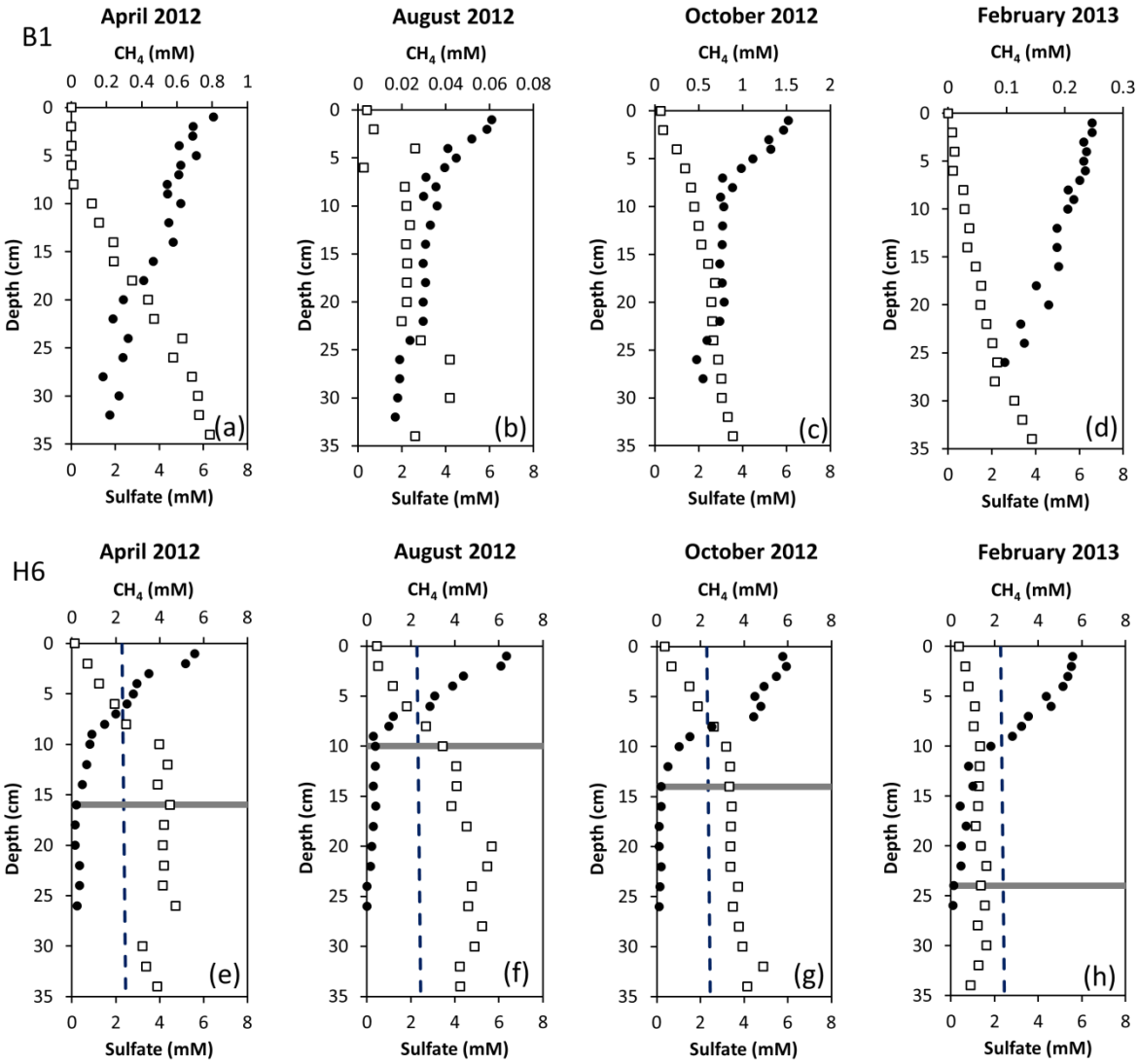

837

Figure 2. Porewater profiles of total methane and sulfate at station B1 (a-d) and station H6 (e-h) for the different sampling periods. The grey line marks the maximum depth of sulfate penetration. The dashed lines indicate the methane saturation concentration at 1 atm pressure (grey) at the time of sampling. All concentrations of methane are below the in situ saturation concentration of methane (see text for details).

838

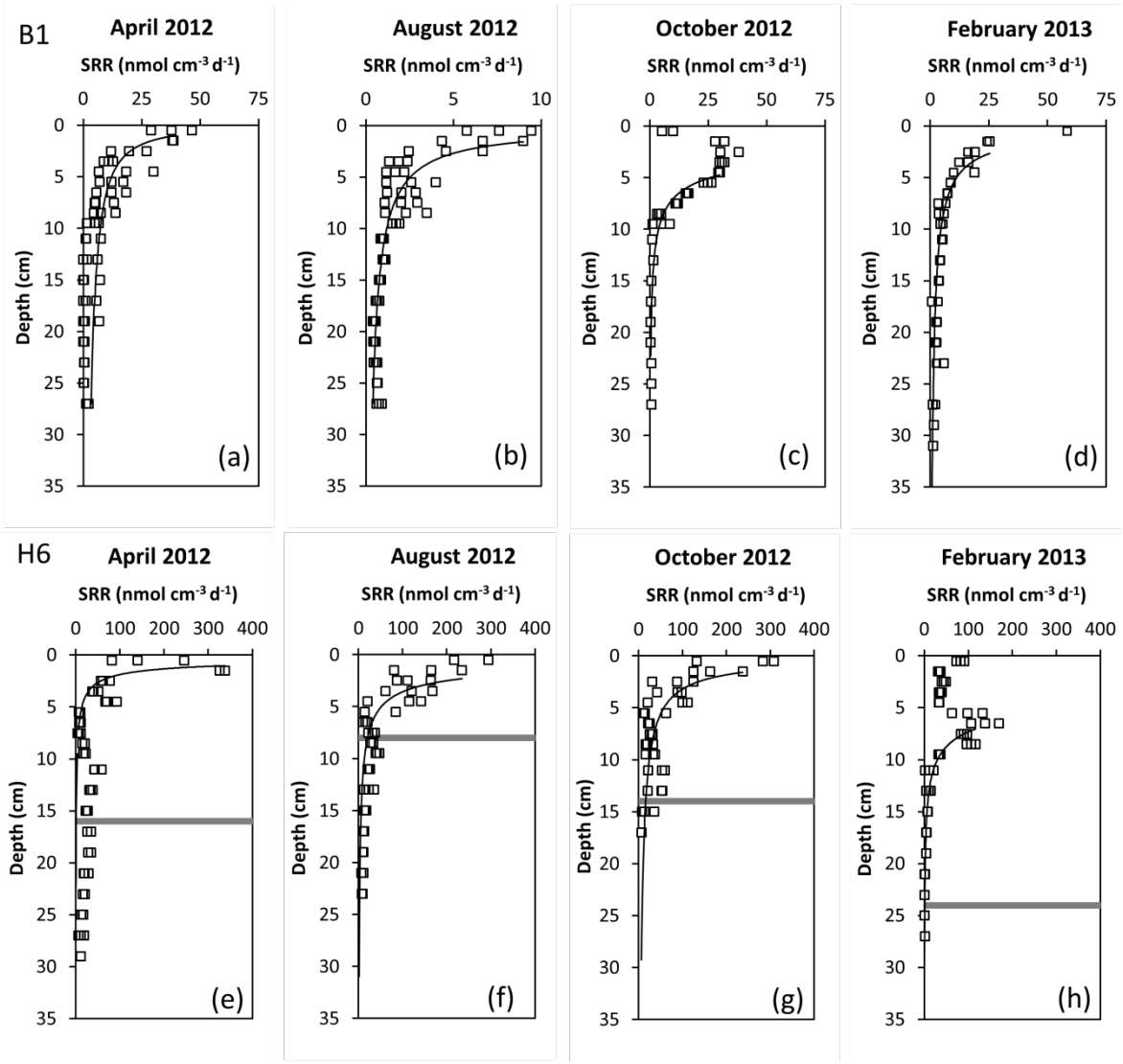

839

840

Figure 3. Depth gradients of bacterial sulfate reduction rates (SRR) measured with ^{35}S-sulfate at station B1 (a-d) and station H6 (e-h) for the different sampling periods. Black lines show the regression results to a power function of the form $y = ax^{-b}$. The grey line marks the maximum depth of sulfate penetration.

841

842

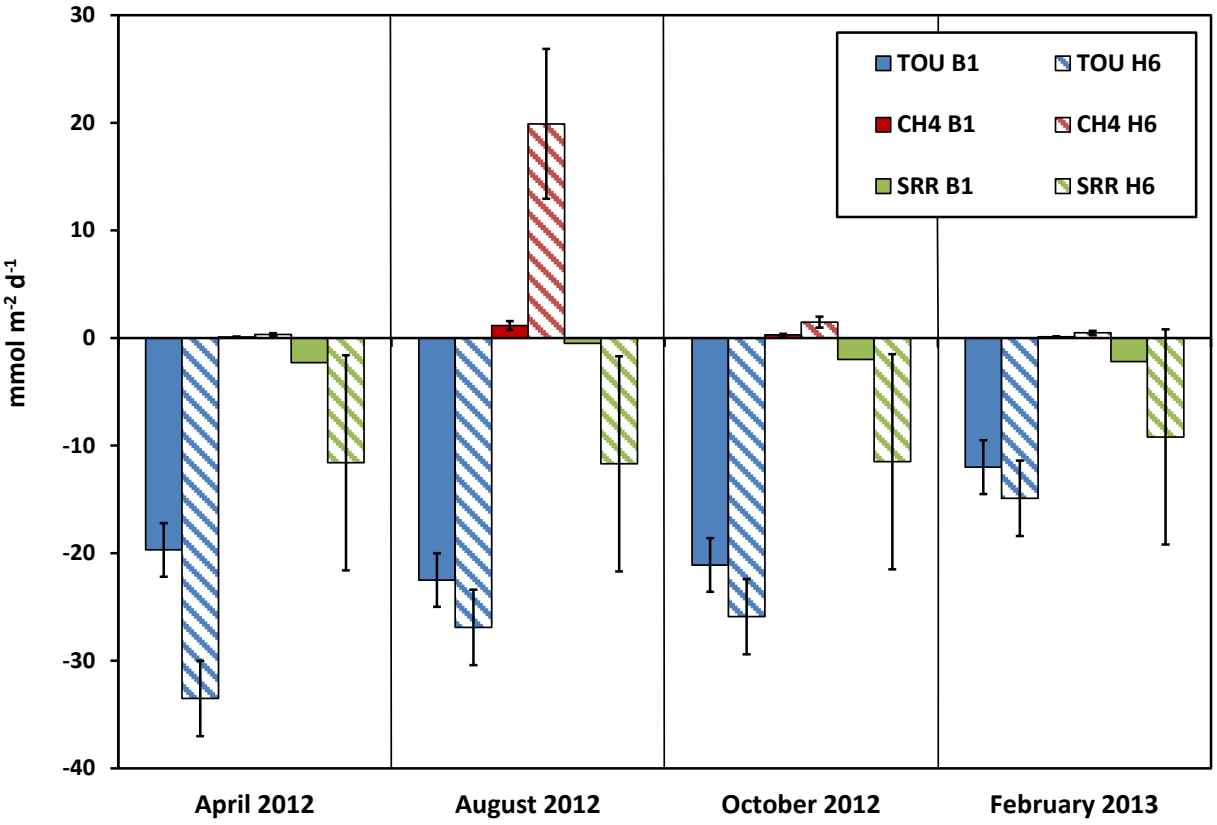

843

Figure 4. Comparison of benthic fluxes (mmol m^{-2} d^{-1}) for sulfate (SO_4), methane (CH_4), and oxygen (TOU) for the different sampling periods.

844

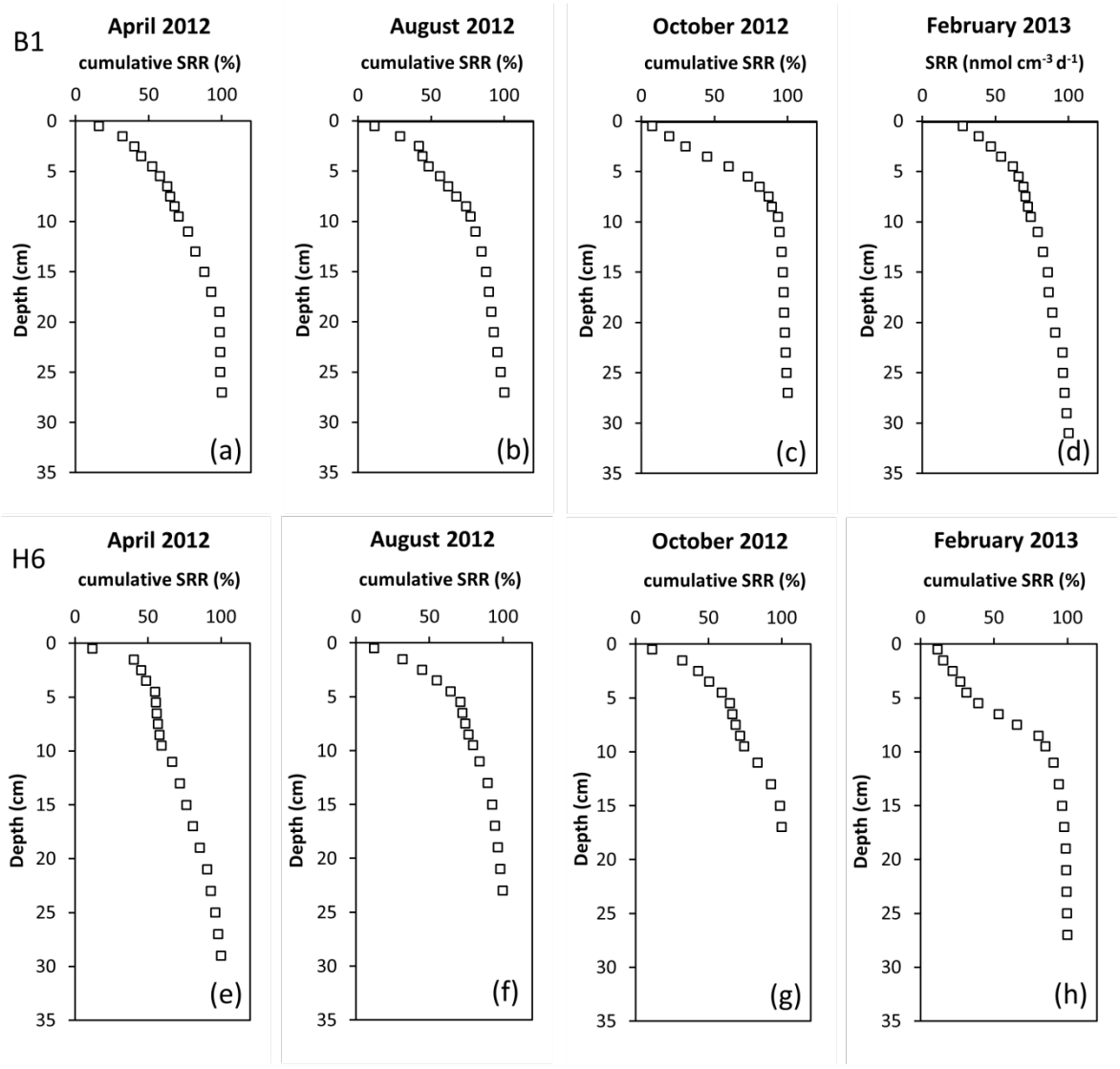

Figure 5. Depth distribution of sulfate reduction rate expressed as cumulative percentage at station B1 (a-d) and station H6 (e-h) for the different sampling periods. The grey line marks the maximum depth of sulfate penetration.